

Prognostic-Enabling of an Electrohydrostatic Actuator (EHA) System

Sonia Vohnout¹, David Bodden², Byoung Uk Kim³, Robert Wagoner⁴, Neil Kunst⁵, Patrick Edwards⁶, Bill Gleeson⁷, Dennis Cascio⁸, Steve Brzuszkiewicz⁹, Roy Wagemans¹⁰, Matthew Rounds¹¹, and N. Scott Clements¹²

^{1,3,4,5,6,7,11}*Ridgetop Group, Inc., Tucson, AZ, 85741, USA*

svohnout@ridgetopgroup.com
tkim@ridgetopgroup.com
rwagoner@ridgetopgroup.com
nkunst@ridgetopgroup.com
pedwards@ridgetopgroup.com
bgleeson@ridgetopgroup.com
mrounds@ridgetopgroup.com

^{2,11}*Lockheed Martin Aerospace, Fort Worth, TX, 78744, USA*

david.s.bodden@lmco.com
scott.clements@lmco.com

^{7,8}*Moog, Inc., East Aurora, NY, 14052, USA*

dcascio@moog.com
sbrzuszkiewicz@moog.com

⁹*Dell Services (Netherlands), 1014 AK Amsterdam, Netherlands*

Roy_Wagemans@Dell.com

ABSTRACT

A proof-of-concept prognostic solution for certain failure modes in the power electronics that drive the flight-critical F-35 Joint Strike Fighter (JSF) electrohydrostatic actuators (EHA) is presented. This program was led by Ridgetop Group under U.S. NAVAIR Small Business Innovation Research (SBIR) funding, and included Lockheed Martin Aeronautics Company (LM), Moog, and Dell Services (Netherlands). Degradation of the optocoupler that isolates the control electronics from the power electronics was simulated in the lab by physically changing resistance values to alter the current transfer ratio. It is proposed that this degradation would also be indicative of insulated gate bipolar transistor (IGBT) wearout. The experimental approach, the test facility, the data analysis and the findings are discussed. An Off-Board Prognostics Health Management (OBPHM) Demonstrator, developed by Ridgetop Group and Dell Systems and representative of the production OBPHM application currently deployed for the F-35 is described. Implementation considerations and challenges are also discussed.

Sonia Vohnout et al. Copyright 2012 Lockheed Martin, Ridgetop Group, Moog, Dell Services. Reprinted with Permission. This is an open-access article distributed under the terms of the Creative Commons Attribution 3.0 United States License, which permits unrestricted use, distribution, and reproduction in any medium, provided the original author and source are credited.

1. INTRODUCTION

The F-35 electrohydrostatic actuators (EHA) were designed to be maintenance-free, i.e., there were not going to be scheduled maintenance activities for the life of the aircraft. The only repair activities would be associated with identification of faults via built-in test (BIT) or integrated cautions and warnings (ICAW) from system monitors which provide coverage for all critical failure modes. Prognostics have been proposed for some failure modes of the EHA, but not the power electronics unit (EU), which provides the power and control to its associated EHA.

Predicting the future state of health (SOH) of critical components in the EHA system (EHAS) could possibly prevent some loss of mission availability due to unforeseen failures. The objective of this program was to identify the feasibility of assessing the SOH of certain critical components in the EHA power electronics via a novel approach to pre-flight BIT. This approach utilizes frequency-shaped actuator commands during BIT to assess SOH. The program was led by Ridgetop Group under U.S. NAVAIR Small Business Innovation Research (SBIR) funding, and included Lockheed Martin Aeronautics Company (LM), Moog, and Dell Services (Netherlands). Ridgetop Group specializes in electronic prognostic solutions for critical systems. These include sensor array

detectors, harnesses for “prognostic-enabling” critical systems, and analysis software to comprise a complete solution.

As the prime contractor for the F-35 Program, LM’s operational experience with the EHA system and flight control system BIT design was instrumental in defining the data requirements, test plan definition and execution, and assessing the feasibility of integrating diagnostic/prognostic capabilities into the F-35 EHA and the Autonomic Logistics Information System (ALIS).

Moog leads the F-35 EHA subcontractor team which has responsibility for development of the actuators for the primary and secondary flight control surfaces (Figure 1). Moog’s design expertise with the EHA power electronics was utilized to help identify the candidate electronic components that could be artificially degraded during the experiments, and they also provided the test labs and test personnel to conduct the experiments.

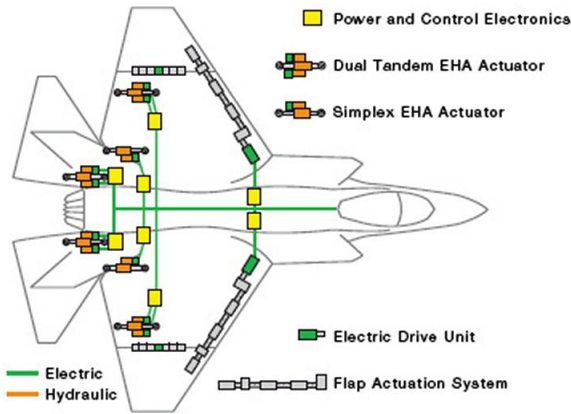


Figure 1. F-35 “Power-by-wire” systems

Dell Services has more than a decade of experience working with Lockheed Martin on the design and development of the Off-Board Prognostics & Health Management (OBPHM) system during the Concept Demonstration and System Design & Development phases of the F-35 program (see Figure 2). This knowledge and experience was used to create a low-cost OBPHM-compatible prognostic demonstrator framework that will be used to present the viability of prognostic capability for the EHA system.

The experimental approach, the test facility, the data analysis and the findings are discussed in the following sections.

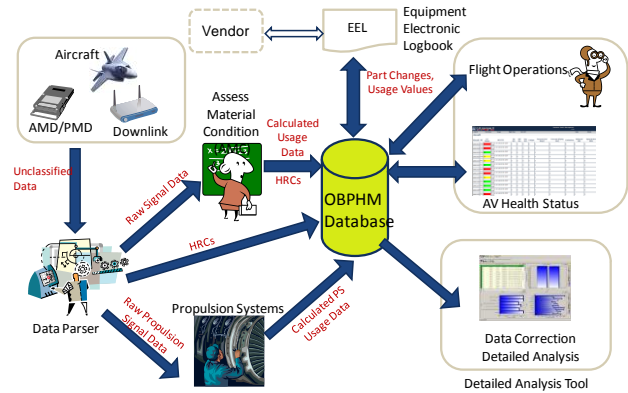


Figure 2. Autonomic Logistics Information System (ALIS) OBPHM system sketch

2. EHA SYSTEM PROGNOSTIC EXPERIMENTS

Various experiments were designed and conducted at Moog’s East Aurora Aircraft Controls facility to characterize fault-to-failure progression (FFP) signatures of the EHA. The original objective was to emulate insulated gate bipolar transistor (IGBT) degradation in the motor drive H Bridge and assess if this degradation could be identified during initiated built-in test (IBIT) by examination of the actuator response to an input command. However, since the servo drive IGBTs are typically packaged as a single hybrid module with DC-link and gate drive inputs, along with 3-phase motor drive outputs, it was impractical to vary the high-side collector resistance to directly emulate IGBT degradation. Hence focus was shifted to the more accessible gate driver board and propagation of damage from this isolated low-voltage control circuitry to the high voltage power electronics circuitry.

Our fundamental hypothesis is:

- Degradation or damage to the discrete circuitry surrounding the gate drive logic could result in measurable drift from nominal switch operation.
- Decreased dead-time between high- and low-side device switching could lead to both high- and low-side power transistors in resistive (linear) mode momentarily.
- Excessive power transistor heating accelerates wear and ultimately results in premature end of life.

We then analyzed the gate driver circuitry to identify the components that would affect device switching parameters, be relatively easy to apply synthetic degradation to, and perhaps, be prone to wear. The EHA design utilizes optocouplers to isolate the gate drive circuitry from the PWM controller. Prior research strengthens our basic premise that as damage to the optocoupler accumulates, its ability to deliver switch signals to the IGBT on time may be inhibited. Additionally, the optocoupler circuit includes a series resistor that can easily be modified to synthesize

decreased current transfer ratio (CTR) consistent with damage to the optocoupler's crystalline lattice. Therefore, the optocoupler was selected.

Applying our proven servo drive damage propagation analysis methodology, shown in Figure 3, entails:

- Applying various fault conditions to each critical stage of the servo drive, starting with the gate driver (D1 in Figure 3) and progressing to the power transistors (D2) and motor windings (D3) of each phase.
- Conducting lab experiments to acquire and characterize the pertinent multivariate servo drive data associated with each fault condition and the resulting stress effect on other components in the system.
- Analyzing the FFP signatures of the acquired multivariate data to produce reasoner algorithms that effectively detect precursor events that mark incipient failure of the servo drive subsystem or damage to its individual components.

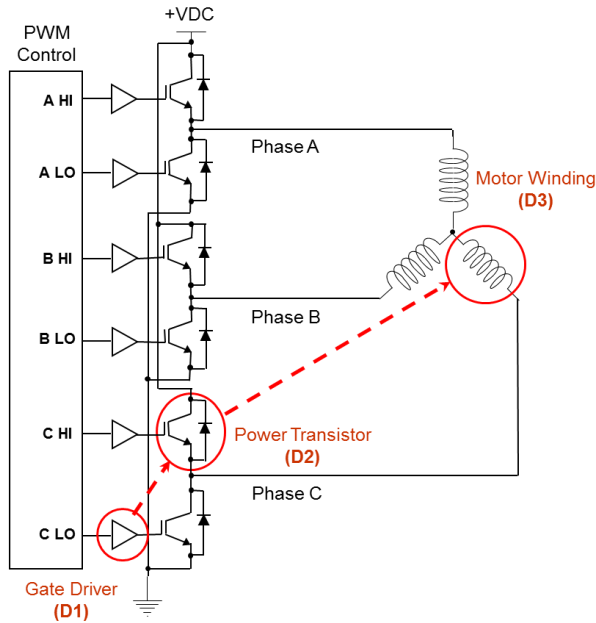


Figure 3. Damage propagation analysis methodology

The optocoupler was synthetically aged by changing the series resistor value to acquire FFP signatures from no degradation to total device failure, under various load conditions. Five different resistance values were utilized to emulate 25%, 50%, 75%, 95% and 100% degradation. The 100% degradation represented a catastrophic collector-to-emitter open circuit fault. The acquired data were recorded in a database and used to develop analysis algorithms to assess the SOH and estimate the remaining useful life (RUL) of the actuator servo drive power electronics.

2.1. EHA System Prognostic Testing

The IBIT and power-up built-in test (PBIT) requirement is that failure detection be designed to detect and isolate greater than 99% of all functional failures within the EHA system. IBIT is executed in two parts, one to test the processing circuitry and the other to verify the drive electronics and the EHA, including the bypass solenoids. These tests are capable of being invoked separately, with the processing circuitry test always engaged prior to the drive electronics/EHA test. The purpose of IBIT is to execute a series of test steps as a means to detect latent system failures that would prevent the system from meeting its reliability and availability requirements. IBIT for the EHA system is invoked by a signal from the vehicle management computer (VMC). IBIT is exited upon a Terminate IBIT command from the VMC.

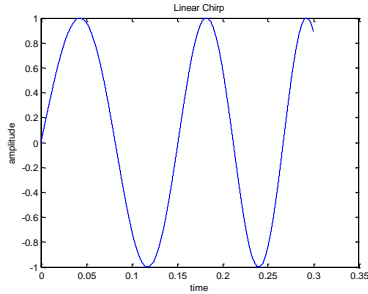
The particular test that would lend itself to evaluation of the frequency response characteristics consistent with the goals of the test program would be the EHA rate test.

The duplex actuators on the flaperon and horizontal tail each have dual pumps and motors that are tested. In addition, there is triplex redundancy in the control electronics (two physical, one model) for each pump/motor. Consequently, six maximum rate command tests are run.

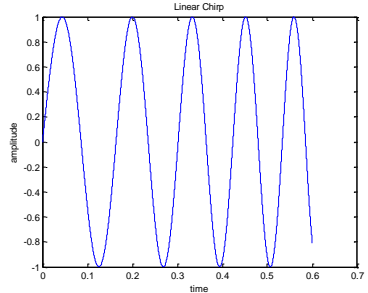
The critical item is the amount of time available for each of the six tests. It can be calculated that there is approximately a 300 msec time allocation for each of the six max rate commands. There is a total maximum time allocation to IBIT for the EHAS so any dynamic movement of the surfaces should be kept to less than 300 msec as a target value for each of the six tests.

In order to maximize the prognostic signature available during IBIT, different types of frequency shaped actuator motion profiles were tested. These included: 1) a chirp type of sine sweep command, and 2) a sinusoidal input at a selected frequency. The bandwidth for these sinusoids was chosen at the upper end of the frequency response capability for the actuators in order to maximize the number of sinusoids in the motion profile. For the chirp signals, this was initially selected to be a 5.5 to 10 Hz frequency sweep. The waveforms for a linear chirp for a 300 and 600 msec time period are illustrated in Figure 4(a) and Figure 4(b), respectively. The 600 msec waveforms were utilized in the test program to identify any improvements to the prognostic signature that could be obtained with more sinusoids in the stimulus.

An exponential chirp waveform for a 5.5 to 10 Hz frequency sweep is illustrated in Figure 5(a) and Figure 5(b) for a time period of 300 and 600 msec, respectively. For this limited frequency sweep and time, there is not a significant difference in the waveforms between the linear and exponential chirp signal.

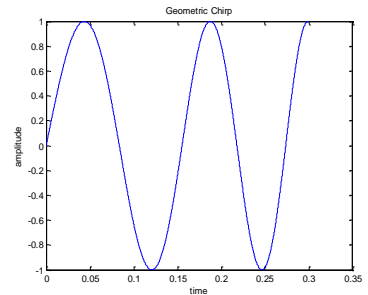


(a) 300 msec, 5.5 to 10 Hz

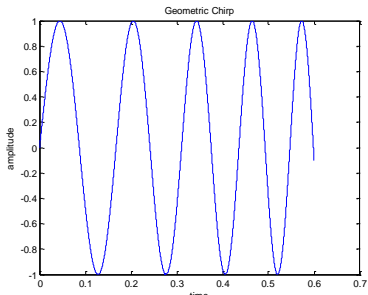


(b) 600 msec, 5.5 to 10 Hz

Figure 4. Linear Chirp Waveforms



(a) 300 msec, 5.5 to 10 Hz



(b) 600 msec, 5.5 to 10 Hz

Figure 5. Exponential signal waveform

2.2. Experiments Overview

The Moog test facility in East Aurora, New York was utilized to conduct the experiments. The lab setup is

illustrated in Figure 6 through Figure 8. This includes the flaperon EHA, shown in Figure 6, the power drive electronics (PDE) unit shown in Figure 7, and the integrated test computer (ITC) in Figure 8.

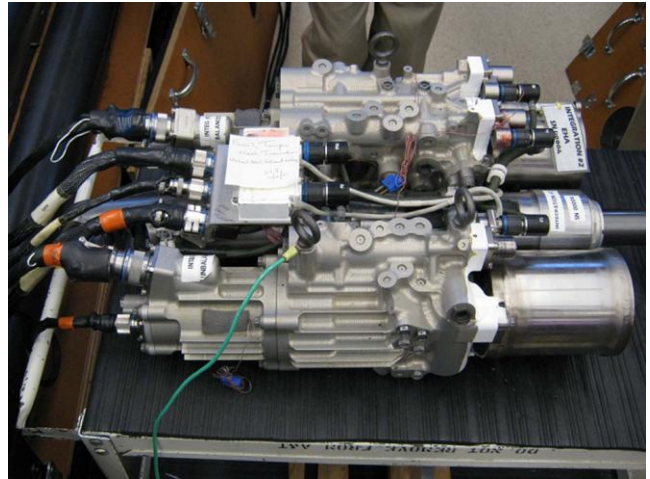


Figure 6. Flaperon EHA used in experiments

The PDE shown in Figure 7 is where the fault-seeded gate driver circuit is housed. Oscilloscope probes, visible on the left side of the PDE, are monitoring the gate driver output.



Figure 7. Power drive electronics (PDE) unit

The ITC shown in Figure 8 controls the operation of the test stand and downloads data from the digital recorder. Motion profiles and test stand digi-rec (digital recording) commands are configured from this workstation.

Figure 9 shows a portion of the gate driver circuit schematic, which was the source of fault seeding. As previously mentioned in Section 2.0, different resistor values were placed in the input diode’s cathode branch to simulate degradation of the optocoupler. The resistor values were changed by physically removing a resistor and soldering in a new one with the specified ohmic resistance.



Figure 8. Integrated test computer (ITC)

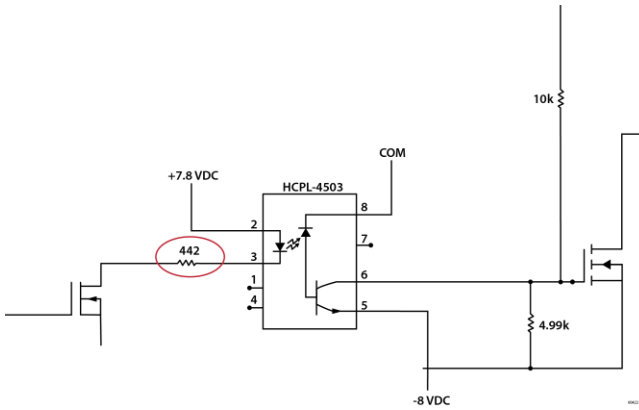


Figure 9. The gate drive circuit with R_{gd} (gate driver resistor) circled in red

Five different levels of degradation were chosen, simulating an even decline in health from nominal degradation to terminal failure. Note that the actual degradation percentages are slightly different from the previously stated values due to the available resistor characteristics.

| Hardware Config. | Actual Degradation | R_{gd} (ohms) |
|----------------------|--------------------|-----------------|
| Baseline | 0% | 442 |
| Degradation 25% | 25.70% | 681 |
| Degradation 50% | 55.10% | 953 |
| Degradation 75% | 76.30% | 1150 |
| Degradation 95% | 95.70% | 1330 |
| Terminal Degradation | 100% | 1370 |

Table 1. Gate driver configurations

2.3. Motion Profiles

It was determined that the best plan of action was to collect baseline data for each individual motion, and then string

them into a composite motion of appropriate length to improve test and analysis efficiency. A detailed summary of the motion profiles is shown in Table 2.

| Motion | Signal | Frequency – Hz Max Velocity (°/sec) | Duration (msec) | Amplitude (In.) |
|--------|-----------------|--------------------------------------|-----------------|-----------------|
| 1 | Run | 54° / sec | 560 | 3 |
| 2 | Step (50% duty) | 60° / sec | 500 | .3 |
| 3 | Sinusoid | 4 Hz | 500 | 0.227 |
| 4 | Sinusoid | 6 Hz | 500 | 0.151 |
| 5 | Sinusoid | 8 Hz | 500 | 0.113 |
| 6 | Linear Chirp | 5.5 -> 10 -> 5.5 Hz 20 ms dead time | 600 -> 300 | Max allowable |
| 7 | Geometric Chirp | 5.5 -> 10 -> 5.5 Hz 20 ms dead time | 600 -> 300 | Max allowable |
| 9 | Linear Chirp | 5.5 -> 10 -> 5.5 Hz 100 ms dead time | 600 -> 300 | Max allowable |
| 10 | Geometric Chirp | 5.5 -> 10 -> 5.5 Hz 100 ms dead time | 600 -> 300 | Max allowable |

Table 2. Motion description

2.4. Monitored Variables

Several variables were monitored in the test fixture as well as hardware test points inside the gate driver circuit. All software test points were downloaded and all hardware test points were captured with a 2 GS/s oscilloscope.

Table 3 provides a complete listing of collected data points.

| Variable | Sampling Frequency | Test Point | tag | // |
|--|--------------------|------------|---------|----------|
| 270 V internal | 8064 Hz | Software | ITC | #18 A1 |
| 270 V Bus Link Capacitor Voltage | 8064 Hz | Software | ITC | #19 A2 |
| Phase A Motor Current | 8064 Hz | Software | ITC | #110 A3 |
| Phase B Motor Current | 8064 Hz | Software | ITC | #111 A4 |
| Phase C Motor Current | 8064 Hz | Software | ITC | #112 A5 |
| Commanded Position (inches) | 80 Hz | Software | ITC | #113 A6 |
| Actuator Position (inches) | 560 Hz | Software | ITC | #117 A7 |
| Actuator Velocity (rad/sec) | 2240 Hz | Software | ITC | #118 A8 |
| Local Motor Velocity CMD | 560 Hz | Software | ITC | #119 A9 |
| Quadrature Axis Current Error | 8064 Hz | Software | ITC | #120 A10 |
| Phase A Gate Driver Command (GATE_DVR_A_OUT) | 2 Gs/s | Hardware | O-Scope | Scope 1 |
| Phase A IGBT Gate (G2_A) | 2 Gs/s | Hardware | O-Scope | Scope 2 |

Table 3. Monitored test points

3. DATA ANALYSIS

A significant amount of data was collected during the testing. Approximately 2.4 gigabytes of data were collected through the course of 72 trials. Each motion profile that was tested was recorded three times for repeatability analysis. The data analysis methodology uses data collected while running a composite motion profile with different resistor values, as previously shown in Table 1.

3.1. Analysis Methodology

Data collected with a resistor value of 440 Ω is used as the “golden,” “healthy,” or “reference” data. The goal of this data analysis methodology is to create a signature that can be used to compute the level of degradation of any future test runs. This methodology computes differences from the

golden signature and sums the differences over time. The summed differences relate to fault degradation. The fault degradation is used to determine a fault-to-failure progression.

The algorithm flow of extracting signatures from a data set is described in Figure 10. There is a basic assumption that there is both a nominal data set and a fault-seeded or degraded data set. There is also an assumption that the degraded data sets are ordered in increasing levels of degradation. We begin with the “golden” data set. Each data set (nominal and degraded) is made up of a certain number of measured parameters, recorded at a certain frequency over a certain time interval.

```

1: For golden data set,
2:   For each time i,
3:
4:
5:   _____
6:   End For
7: End For
8: For each degraded data set,
9:   For each time i,
10:    For j = 1;3, _____
11:
12:   End For
13:   _____
14: End For
15: For each windows, T
16:
17: End For
18: Compute a minimum gap
19: Compute the maximum of the minimum gap
20: End For
    
```

Figure 10. Analysis methodology procedure

A brief explanation of the analysis methodology to identify the actuator motion profile that provided the best prognostic signature follows. From Line 1 to Line 6, three amplitude values and a middle value m_i is calculated from three amplitude values for each time in the golden data set. This means that the nominal data set produces a total of n middle values where n is the number of golden data sets. From Line 8 to Line 14, a degraded data set is considered, and an intermediate distance value, $D_{T,k}$, and the average of the three intermediate distance values, $\bar{D}_{T,k}$, are computed, where k refers to the degradation level. Thus a total of n average intermediate values are computed for each level of degradation. From Line 15 to Line 17, the final average of the distances is computed from the data set consisting of n time values. A window size is chosen of w time values where w is less than or equal to n . This produces T final

averages for each of the degraded data sets. Last, we find the maximum of the minimum gaps. A minimum gap is generated by first calculating the difference between the final average for successive degradation levels, $D_{T,k} - D_{T,k-1}$. A total of $k-1$ differences are determined, one less than the total number of degradation levels. The minimum gap is the minimum of these differences and indicates the distances from the nominal relative to degradation. **The maximum of the minimum gaps provides the right edge of the time window T corresponding to the signature.** This tells you where there is a good separation of the means of the measured parameters that correspond with degradation. Figure 11 shows the maximum of the minimum gaps in green, motion profile in black, and best signature time in red.

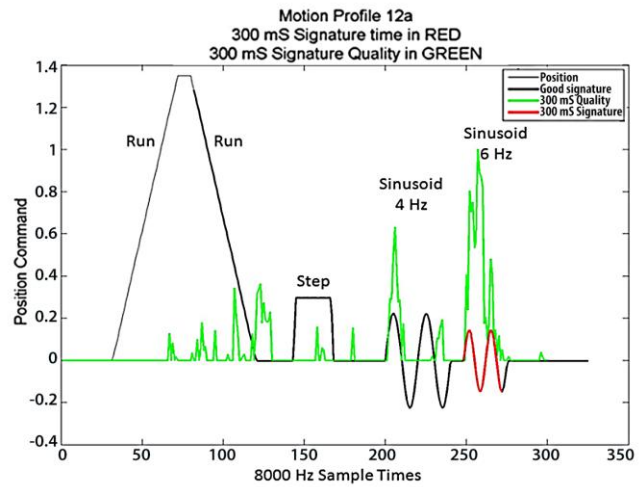


Figure 11. 300 ms signature search motion profile

The application of the methodology identified the quadrature axis current error (QACE) data signal (see Figure 12) as the best failure precursor when combined with a simple 6 Hz sinusoidal motion profile.

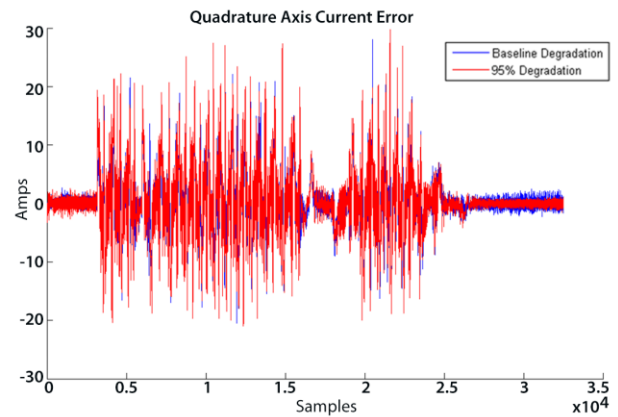


Figure 12. Quadrature axis current error (QACE)

The initial data analysis methodology used all of the data collected at 8 kHz. However, since data are written to the VMS bus in the aircraft at only 80 Hz, the prognostic analysis methodology would need to work at this data rate. Consequently, the analysis was performed again with the data decimated down to 80 Hz. The results are illustrated in Figure 13.

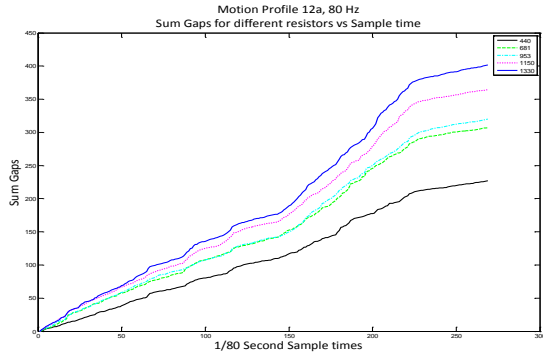


Figure 13. Total sum_gaps for 80 Hz samples

After the QACE 8 KHz data from all test runs were decimated to 80 Hz, the search for the maximum of minimum gaps produced the same signature as shown in Figure 11 above.

The fault-to-failure signature utilizing the analysis methodology applied to the QACE data is plotted in Figure 14 for all resistor values: 440 Ω (○), 681 Ω (□), 953 Ω (■), 1150 Ω (◇), and 1330 Ω (×). This plot illustrates the increasing prognostic signature as the synthesized degradation increases.

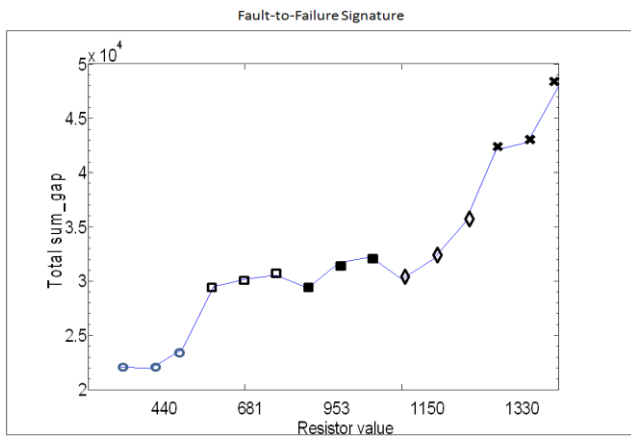


Figure 14. Total sum

SOH assessment is calculated for subsequent tests by comparing the subsequent test measurements with recorded reference signature values. The subsequent total sum gap is compared with totals recorded in the signature file and the SOH is derived by interpolating the new total between the recorded subgaps and percentage degradation for different resistors.

The RUL is calculated from the SOH assessments acquired at various times. A linear RUL estimate is calculated from the assessment times and SOH at the two most recent assessments. The change in SOH per unit of time is assumed to be a constant. The RUL is a linear extrapolation of the two most recent states of health and assessment times. More accurate RUL is attainable by monitoring SOH degradation over real time on a real system.

4. OFF-BOARD PHM DEMONSTRATOR AND REASONER FACTORY

The work on the PHM Demonstrator consisted of establishing the system engineering tasks and activities required for the design of a signal parser and OBPHM Demonstrator. Dell Services provided domain knowledge, software engineering, and business process expertise required to design the OBPHM Demonstrator such that future integration of algorithms into production systems is realistic.

The flow depicted in Figure 15 represents the path the data follow from on-board to off-board systems for processing. The data are taken off the aircraft by means of a portable memory device. The unclassified PHM and signal data are split off from the classified data and transferred to the OBPHM system, which calculates, tracks, and visualizes RUL of various components. Additionally, maintenance work orders can be generated for repair and replace actions as needed. The rationale for the approach that was taken to minimize costs associated with transferring technology from a research and development to a production environment is self-explanatory. To achieve the highest possible level of compatibility between the concept demonstrator and the production OBPHM system, software components were developed with functionality similar to that in a production environment. Also, the same software development toolset that Dell used to support OBPHM development was used for this work.

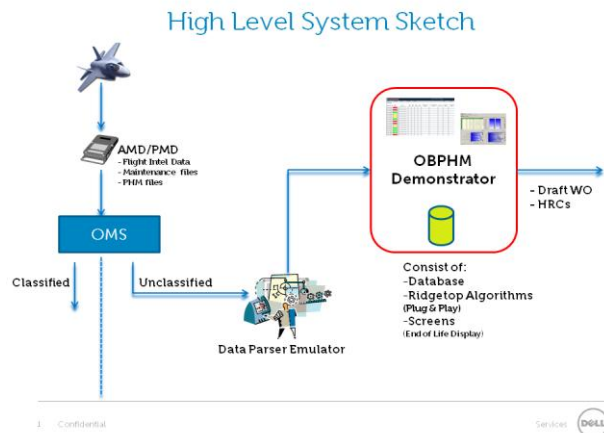


Figure 15. System sketch

The tools developed are outlined in Table 4:

| Requirements Tools | |
|--|---|
| Starteam | http://www.borland.com/us/products/starteam/ |
| Modeling Tools | |
| Together Control Center 2007 | http://www.borland.com/together/ |
| XML Spy | http://www.xmlspy.com/ |
| Configuration Management Tools | |
| Subversion | http://tortoissvn.tigris.org/ |
| Database Tools | |
| Oracle | http://www.oracle.com/ |
| Toad Oracle (Tool for Database Administrators) | http://www.toadsoft.com |

Table 4. System design tools

The Demonstrator Software Prototype and Data Parser Software Emulator Prototype runs in a single environment for demonstration purposes. A distributed architecture was not developed as part of the initial capability. Figure 16 represents the architecture for the Demonstrator. The EHAS architecture consists of components and interfaces and supports loose coupling. Each component implements a single related set of functionality.

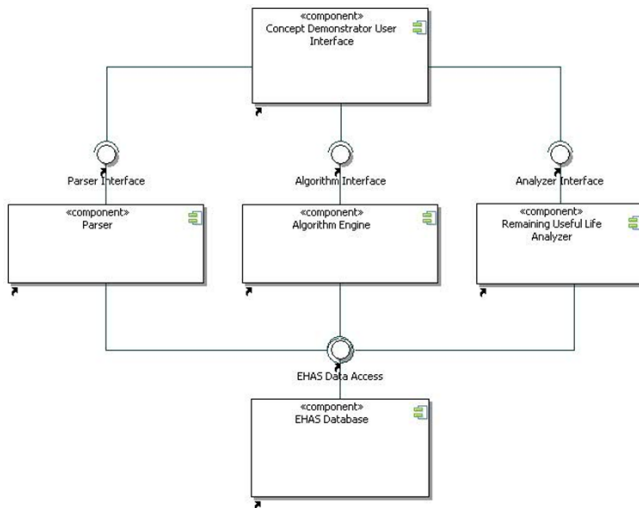


Figure 16. Demonstrator overview

The EHAS architecture consists of the following components:

- **Concept Demonstrator User Interface:** This component represents the interface to the end user for interaction with the Parser component, Algorithm Engine component, and the RUL Analyzer component.
- **Parser Component:** The Parser component has the capability to parse datasets, offers the capability to view the parse results, and the ability to delete these results.

The Parser component has a Parser Interface, which is utilized by the Concept Demonstrator UI component.

- **Algorithm Engine Component:** The Algorithm Engine component has the capability to run algorithms and to view the run results. The Algorithm Engine component has an Algorithm Interface, which is utilized by the Concept Demonstrator UI component. The algorithm engine also ensures that parsed data sets are processed in chronological sequence.
- **Remaining Useful Life (RUL) Analyzer Component:** The RUL Analyzer component offers the capability to view the RUL analysis and has an Analyzer Interface, which is utilized by the Concept Demonstrator UI component.
- **EHAS Database:** The EHAS Database component offers a Data Access Interface to the other components to view, create, update, and delete data required by the various Concept Demonstrator functions.

The architecture puts in place the basic framework of being able to parse signal data, process parsed data, and display RUL. More work is needed to make the system more robust. For example, as we learn more of the performance characteristics of the air vehicle it may be necessary to recalculate remaining life of one or more components. Flight/system data are stored starting, in some cases, during production. There can be cases where all the flight data need to be reprocessed starting from day one or some other point in time during the life of the aircraft.

This basic design principle introduces additional complexity. For example, it does not make sense to recalculate remaining life for components that have already been scrapped. Also, parts may be refurbished, returned to the supply chain and end up on a different aircraft from the first install; the component may even end up on an aircraft belonging to a different country's air force. Therefore the OBPHM system needs to be able to track which component was installed on which air vehicle and the period of time that it was installed. Additionally, it is essential that Performance-Based Logistics contracts are put in place with partner nations or we may not be able to feed the system all the needed flight and performance data to effectively perform prognostics and health management. PHM and remaining life data accompany the component throughout its life so for each period that a component is "on wing" it is known what its start and end RUL characteristics were.

Finally, as the aircraft matures over time, changes will be incorporated. For the PHM demonstrator the signal definitions are most important, as this is a configuration-managed item. So it is not enough to know which part flew in which air vehicle for a given flight of the air vehicle. We must also be able to determine the correct set of signal definitions that are an essential input to the parser function.

Since we expect to tighten tolerances used in the PHM algorithms as the air system matures, it is essential that algorithms do not require to be recompiled with version updates to the OBPHM system. Many copies of the OBPHM system run in multiple locations and countries. Version updates of the OBPHM software are therefore not trivial and are time-consuming to roll out. Hence the design requirement for PHM algorithms to be parameter-driven, which in the current version of the demonstrator they are not.

4.1. Reasoner Development

For the final demonstration, two reasoners were successfully developed and integrated with the OBPHM demonstrator, using the supplied test run datasets presenting both the SOH and RUL. In addition, the system was able to repeatedly discover the signatures of interest as the data were decimated from 8 kHz down to 80 Hz, proving that the same algorithm without change could detect the degradation with fewer data points. Figure 17 and Figure 18 show the final EHAS concept demonstrator using the datasets at 80 Hz with a 300 ms detection window for SOH and RUL.

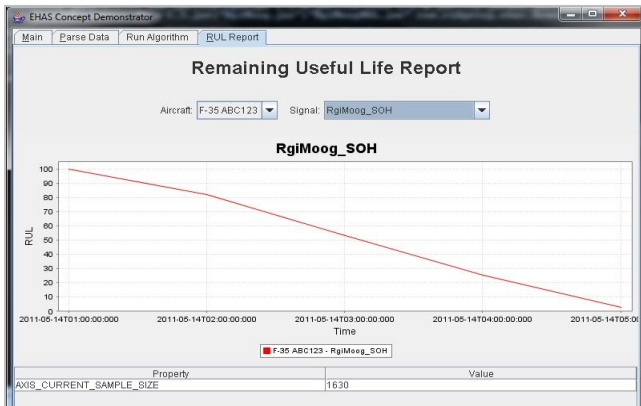


Figure 17. Results SOH report screen

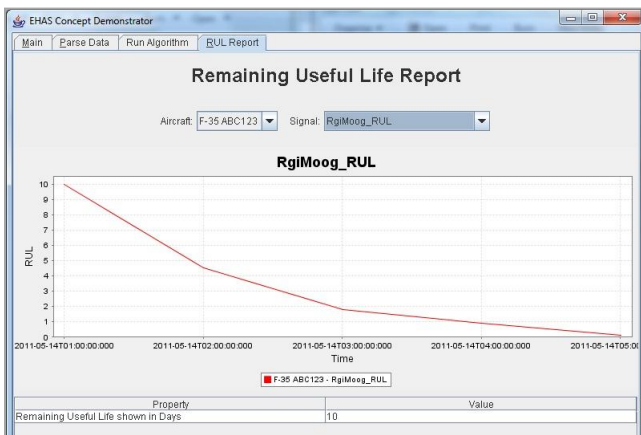


Figure 18. Results RUL report screen

5. PROGNOSTIC ARCHITECTURE AND IMPLEMENTATION CONSIDERATIONS

The essential idea of the prognostic methodology presented in this paper is to sum the absolute value of the difference between a degraded signal and a golden (reference) signal. The gaps or differences between different levels of degradation are then computed and the running sums again calculated to obtain sum_gaps. An average gap is then computed to be used as an indicator of the strength of the prognostic signal. The implementation of two error summations essentially applies a “magnifying glass” to the differences between the degraded signals and the reference value so that the best failure precursor signal, on a relative strength level, can be identified.

The application of this methodology identified the QACE as the data signal that provided the best failure precursor when combined with motion profile 4, a 6 Hz sinusoidal motion.

5.1. Prognostics Architecture Feasibility

There are two primary factors in going forward with technology implementations on the F-35. The first is technical feasibility, and the second is return on investment (ROI). By ROI, we essentially mean that the technology has to earn its way on the aircraft by providing a cost benefit that will result in net cost savings over the life of the program.

5.1.1. Technical Feasibility

The F-35 vehicle systems network (VSN) is the primary means for transfer of data between vehicle system subsystems and components. This includes transfer of data between the VMCs and the EHA EU.

The lab experiments and data analysis indicated that a prognostic algorithm to calculate RUL for a degraded optocoupler is feasible for this particular failure mode when tested in a lab environment. The key question is how would the algorithm perform in an operational environment? Since the motion profile would be implemented during IBIT, which would provide a somewhat repeatable field environment, variability in the EU states and resulting effect on the prognostic algorithm would be minimized. The concern is then the effects of noise and other environmental factors such as temperature on the QACE signal and RUL calculations.

Temperature variations could have a significant effect at the extremes of the operational environment. It is highly probable that the EU behavior would be significantly different at -20 °C than at 23 °C due to lower fluid temperatures requiring more power input to the motor. Temperature and resulting power variations and their effect on the QACE would have to be considered in the prognostic algorithm.

Variations in signal strength or noise due to other external sources such as variability in components would most likely have to be compensated for. The strategy computes SOH utilizing the sum_gaps obtained from the laboratory testing based on field data obtained during IBIT. The RUL could then be inferred from the current sum_gap value and its rate of change and projected time to reach the 100% degradation value. However, since the sum_gap is essentially a “double summation” over time of the errors from the golden values, variations in noise could produce significant deviations from the sum_gaps established in the laboratory testing. This is illustrated in Figure 19. Four levels of random, Gaussian, zero-mean noise were simulated (with standard deviations of 0.1, 1.0, 3.0, and 5.0). Note that the Iq deviation values have an amplitude mostly less than 10 A. The chosen noise signals thus have standard deviations ranging from 1% to 50% of the amplitude of the signal. The blue line represents the sum gap between the 681 and 440 ohm resistance values, the green line between the 953 and 440 resistance values, etc. There are two reference levels on the plot, one with the reset function (dashed horizontal colored lines), and one without (solid colored horizontal lines). The one without is the reference value of interest since the reset function is neither necessary nor desired for a prognostics implementation based on IBIT data.

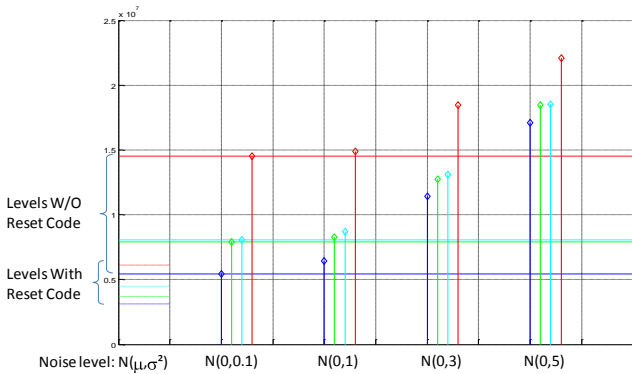


Figure 19. Effect of noise on Sum_Gap calculations

Would the QACE signal have much variation due to noise or temperature? We do not know the answer to that. But as the plot illustrates, even with a standard deviation of 1, significant errors in the reference values used to estimate RUL would be incurred. Consequently, this would have to be monitored.

5.1.2. Return on Investment (ROI)

In order to justify implementation of a prognostic algorithm for the EHAS EU, it has to address a significant issue that could affect the operational costs and mission availability of the fleet. Performing prognostics for the optocoupler only would most likely not meet those criteria. The question is which other failure modes in the EU would also show up in the QACE signal? Another question is how would you isolate between an IGBT failure mode or optocoupler failure

mode or any other failure modes that would affect the QACE signal? Different failure modes would most likely have different sum_gaps associated with their remaining useful life calculations. Distinguishing between failure modes would most likely require data fusion of different signals, and lab data to establish sum_gap levels associated with failure.

6. CONCLUDING REMARKS

The laboratory testing at Moog on a simulated optocoupler failure proved to be successful with regard to performing degraded electronic component testing, identifying a motion profile that would fit the severe constraints associated with F-35 IBIT and the VMS architecture, and extracting a prognostic signal that showed progressive degradation commensurate with the induced degradation.

Distinguishing which failure mode might be showing up in the QACE signal is probably a more difficult challenge. This would most likely require a detailed circuit and failure modes, effects & criticality analysis (FMECA) for the power circuitry, and additional degraded component test work to identify a prognostic signature associated with a particular failure mode. A recommendation would be to perform testing on degraded EUs that have been returned due to failures so that a prognostic QACE signature could be established for a known component failure. EUs with failed IGBTs would be a significant opportunity for a test program.

One other strategy for implementation would be to start collecting the QACE signal during IBIT and then monitoring it as a precursor that something is going wrong even if the particular failure mode is unknown. Suggested steps in implementing the methodology are shown in Figure 20.

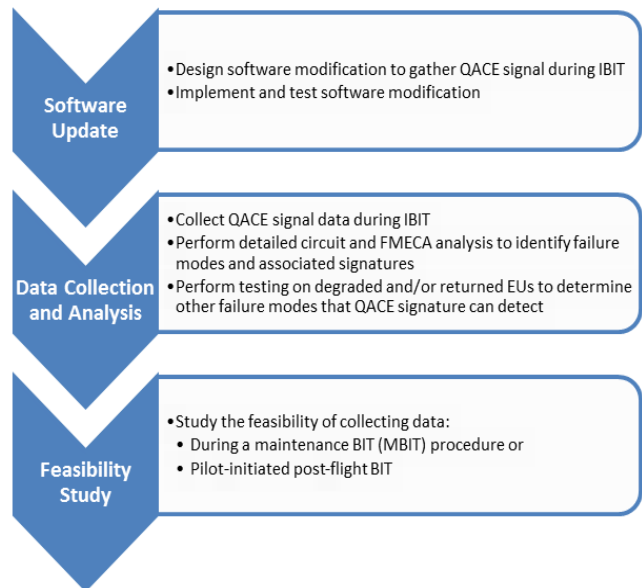


Figure 20. QACE tasks

BIOGRAPHIES

Sonia Vohnout earned her MS in Systems Engineering from the University of Arizona. With a diverse background and experience, Ms. Vohnout is well-suited to manage Ridgetop's Advanced Diagnostics and Prognostics Division as Director. Ms. Vohnout joined Ridgetop Group after successfully building an electronic subassembly business in Mexico, working as a systems engineer at IBM, and handling overseas installations of software with Modular Mining Systems (now part of Komatsu). During her career, she has held executive management and senior technical positions. In addition, she has co-founded several companies. Ms. Vohnout is a board member of the Society for Machinery Failure Prevention Technology (MFPT) (www.mfpt.org), an interdisciplinary technical organization strongly oriented toward practical applications. Ms. Vohnout has published several papers in the field of PHM.

David Bodden is a Senior Fellow at Lockheed Martin Aeronautics Company. His current research is in prognostics for mechanical and electrical systems. Prior to selection as a Fellow, his assignments included six years as Chief of the Control Law design and Analysis Group followed by seven years as the Senior Manager of Flight Control Systems. He has authored numerous papers and technical proposals, and managed numerous technology development programs. He has served on the AIAA Guidance, Navigation, & Control Technical Committee, is former Chairman of the Lockheed Martin GNC Technology Focus Group, is former Chairman of the SAE Aerospace Control and Guidance Systems Committee, and currently serves as Chairman of the Texas A&M Aerospace Advisory Board.

Byoung Uk Kim, Ph.D. is a Principal Research Engineer and a project lead for reliability analysis tool development at Ridgetop Group. The field of interest for his doctoral program was fault detection and root cause analysis systems, electronic prognostics, data mining and data analysis, and self-healing algorithms with autonomic computing. His collegiate repertoire also consists of numerous published papers in reliability analysis and autonomic configuration. Dr. Kim worked on a key NASA reliability/prognostics project in 2006 for Ridgetop. He has contributed to the development of innovative solutions that are currently deployed in the NASA ADAPT program at the Ames Research Center.

Neil Kunst, BSEE and Principal Systems Engineer, has more than 20 years' experience in product engineering, systems engineering, test engineering, logic design, software development, and project management. At Ridgetop he directs the development of the comprehensive prognostics and health management platform, Sentinel Network, which features a distributed software architecture with an embedded sensor network, centralized data collection, advanced reasoning, and asset management of complex mil-

aero systems-of-systems. Mr. Kunst has been recognized by NASA for outstanding performance on ground-breaking research related to electronic power system and electromechanical actuator prognostics.

Patrick Edwards is an Electrical Engineer at Ridgetop Group. He earned his BSEE from the University of Arizona in 2009 and specialized his studies in microcontrollers and embedded system design, computer architecture design, analog and digital control systems, and robotics. Mr. Edwards' undergraduate degree featured advanced studies in system modeling and embedded controller design. He is experienced in electrical and firmware design and integration, as well as PWB layout and embedded systems design. Mr. Edwards played a key role in the successful engineering of a Phase I DOE Small Business Innovation Research (SBIR) program titled "Uptime Improvements for Photovoltaic Power Inverters."

Robert Wagoner is a Senior Software Engineer at Ridgetop Group and longtime member of IEEE. At Ridgetop, Mr. Wagoner has been leading the R&D of Ridgetop's foundation prognostics and health management (PHM) application, Sentinel Network. He is also technical lead on a NASA Phase 2 SBIR program, and is contributing to the commercialization of Ridgetop's MAPR technology and construction of an advanced actuator testbed. He has expertise in robotics development and electric propulsion design for unmanned aerial vehicles. He has developed UAV GNC/IMU-6DOF with GPS and ground station software, and created mainstream use of electric ducted fan-jet models.

Bill Gleeson is a Senior Electrical Engineer at Ridgetop Group. He earned a BS in Engineering Math from the University of Arizona and an MS in Industrial Engineering from Arizona State University. He has six patents and a technical excellence award from PC Magazine. He developed prognostic algorithms for a number of actuator-related programs at Ridgetop Group and found the degradation signature contained in the QACE. Prior to Ridgetop, Mr. Gleeson was VP of Hardware Engineering at NetMedia Inc., and was Senior Scientist at Hughes Aircraft.

Dennis Cascio, MSEE, is a Staff Engineer in the Aircraft Group at Moog Inc. He has over 25 years of experience in power conversion electronics design. Mr. Cascio joined Moog in 2002 after working as a design engineer on switching power supply applications, followed by large industrial AC to DC power conversion systems. At Moog, he has been involved in the design of various motor control power stages including those used in the Joint Strike Fighter, Flight Control Actuation Systems.

Steve Brzuszkiewicz is a Staff Project Engineer in the Aircraft Controls Group of Moog Inc. He has 40 years of experience in the electrical engineering and control system fields. Mr. Brzuszkiewicz joined Moog in 1984 and holds

degrees from Kettering University (BEE) and SUNY at Buffalo (MSEE). At Moog, he has been involved in the design and development phases of flight control and vibration control actuation systems, including those used in the JSF F-35 and B-2 aircraft.

Roy Wagemans is currently Delivery Director for Dell Services and responsible for coordinating Dell's services capabilities in various countries in the EMEA region. Roy has a background in software systems engineering and holds a business degree from the University of Henley. As of 1999 he has held a number of project and program management positions related to the Joint Strike Fighter program all related to the Prognostics & Health Management domain.

N. Scott Clements is a Systems Engineer at Lockheed Martin Aeronautics Company. He is currently researching fault degradation models and associated PHM techniques. He received his bachelor's degree from Mississippi State University in 1996 and his master's and doctoral degrees from Georgia Institute of Technology in 1998 and 2003, respectively. His research interests include PHM, data mining, verification techniques, and fault tolerant control systems.